Supporting information

Device performance improvements in All-Inorganic Perovskite Light-emitting Diodes: the role of binary ammonium cation terminals

Yao Lu[a,b], Jie Dong[a,b], Xiaomin Huo[a,b], Dong Wei[c], Bo Qiao[a,b], Suling Zhao[a,b], Dandan Song*[a,b], Zheng Xu*[a,b]

a Key Laboratory of Luminescence and Optical Information, Beijing Jiaotong University, Ministry of Education, Beijing 100044, China

b Institute of Optoelectronics Technology, Beijing Jiaotong University, Beijing 100044, China

c College of Physics and Energy, Fujian Normal University, Fuzhou, 350117, China.

Address correspondence to E-mail: ddsong@bjtu.edu.cn; zhengxu@bjtu.edu.cn

Table S1 The TRPL parameters for the $CsPbBr_3$ films without (standard) and with phDMADBr modification.

	τ_1(ns)	B_1(%)	τ_2(ns)	B_2(%)	τ_{ave}(ns)
Standard	0.85	68.74	7.96	31.26	1.18
With phDMADBr	2.72	60.68	7.95	39.32	3.67

DFT calculation parameters

The structural optimization and electronic structure calculations were carried out by Cambridge Serial Total Energy Package (CASTEP) in Materials studio. The generalized gradient approximation (GGA) of the Perdew-Burke-Ernzerhof (PBE) functional was employed. The calculation was expanded by using the ultrasoft pseudopotential with a cutoff energy of 517 eV and the total energy was converged to 1×10^{-5} eV. The structural optimization was optimized until the force tolerance on each atom was smaller than $0.03 eV Å^{-1}$, the stress tolerance was smaller than 0.05 GPa, and the displacement tolerance was smaller than 0.001 Å. k-point set were used the Monkhorst–Pack with actual spacing of 0.032 $Å^{-1}$ for structural optimization and electronic property calculations.

CsPbBr$_3$ possesses cubic structure with space group Pm-3m at room temperature with a 3×3×2 supper cell of CsPbBr$_3$. The phDMA^{2+} was placed on the supper cell surface to optimize to convergence.

Table S2 Binding energies and distances of phDMA^{2+} and PMA$^+$ on differently terminated surfaces of CsPbBr$_3$.

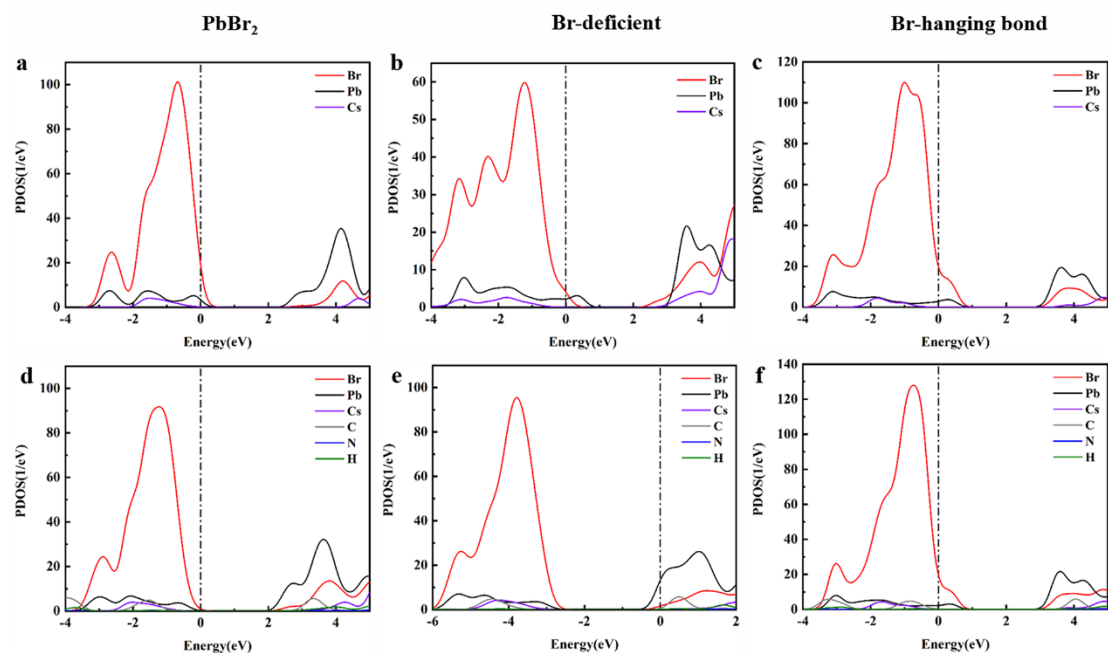| Surface	Binding energy (eV)	Distance (Å)
	phDMA^{2+}	
PbBr$_2$	-6.10	2.73
Br-deficient	-9.04	2.65
Br-hanging bond	-16.94	2.25
	PMA$^+$	
Br-hanging bond	-12.49	2.23

Figure S1 (a-c) Partial densities of states (PDOSs) for the PbBr$_2$, Br-deficient, and Br-hanging bond surfaces of CsPbBr$_3$. (d-f) Corresponding results with phDMA^{2+} attached.
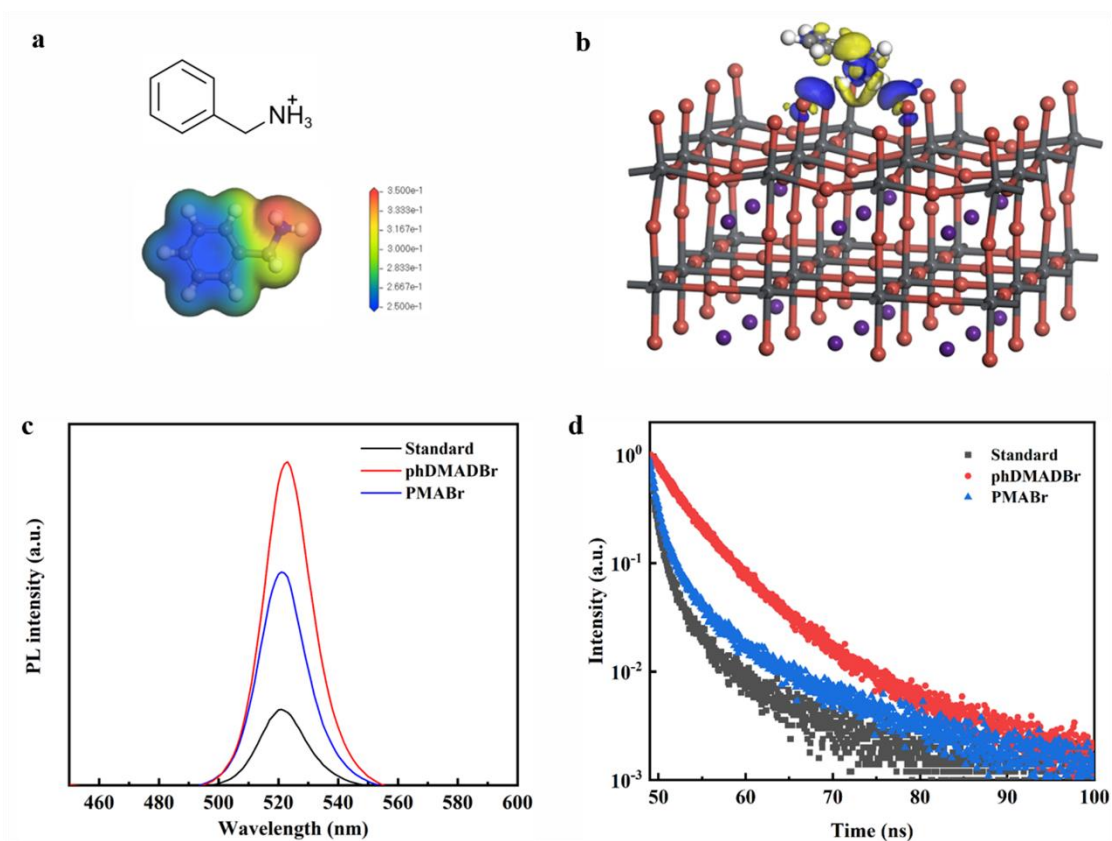
Figure S2 (a) Chemical structure (top) and electrostatic potential map (bottom) of the PMA$^+$ ion. (b) Electron density differences for the PMA$^+$ ion on the Br-hanging bond surfaces of CsPbBr$_3$. (c) PL spectra, and (d) TRPL decay curves of the CsPbBr$_3$ films without (standard), with phDMADBr and with PMABr modification.
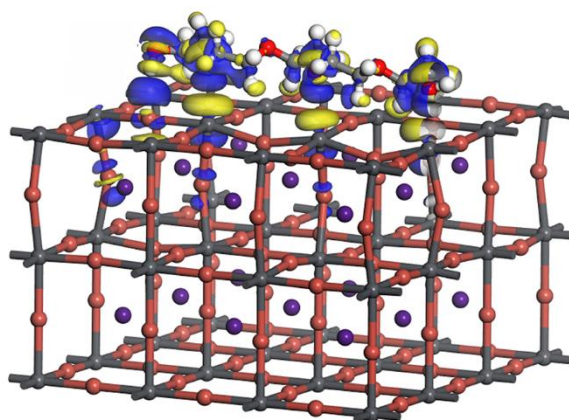

Figure S3 Electron density difference for the PEG on the PbBr$_2$ surfaces of CsPbBr$_3$. Due to the worse quality of the all-organic films, the pure CsPbBr$_3$ PeLEDs with a non-ideal performance. A small ratio of PEG added in perovskite can enhance the device performance in previous reports. We

use the PEG-CsPbBr$_3$ PeLEDs as our basic device, and explain the different passivation mechanisms of PEG and the ion additives in this work. Through the results in this work, the binding energy and electron density differences show that the interaction between aryl ammonium ion and CsPbBr$_3$ were mainly worked by the NH$_3^+$ terminal and Br-hanging bond surfaces. The electron density difference was calculated by DFT between PEG and CsPbBr$_3$ (shown in **Figure S3)**. Obviously, the interaction between them mainly occurs through the lone pair electrons of oxygen in PEG and Pb^{2+} of the CsPbBr$_3$ surface. PEG and the aryl ammonium ion possess different passivation mechanisms and both have obvious effect to the all-inorganic perovskite.
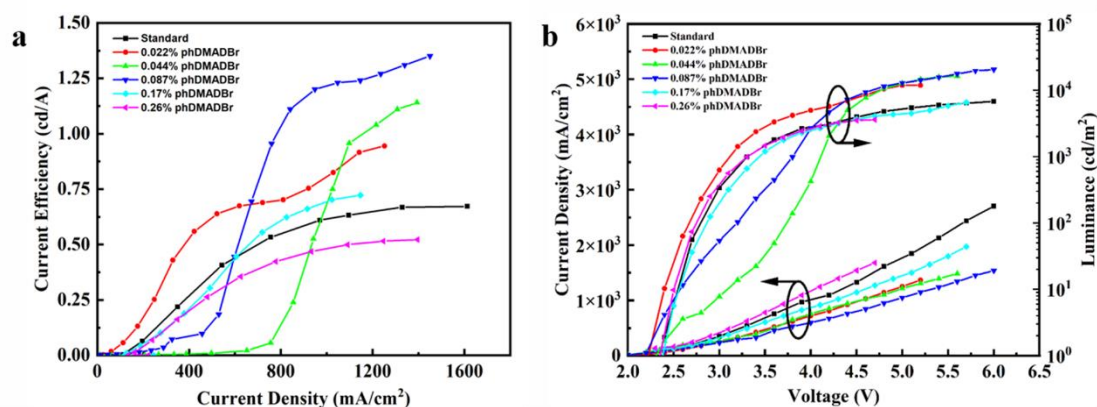

Figure S4 (a) Current density-voltage-luminance curves and (b) current efficiency-current density curves of the PeLEDs modified with different concentrations of phDMADBr.

Table S3 Device characteristics of CsPbBr$_3$ PeLEDs without (standard) and with different concentration phDMADBr modification.

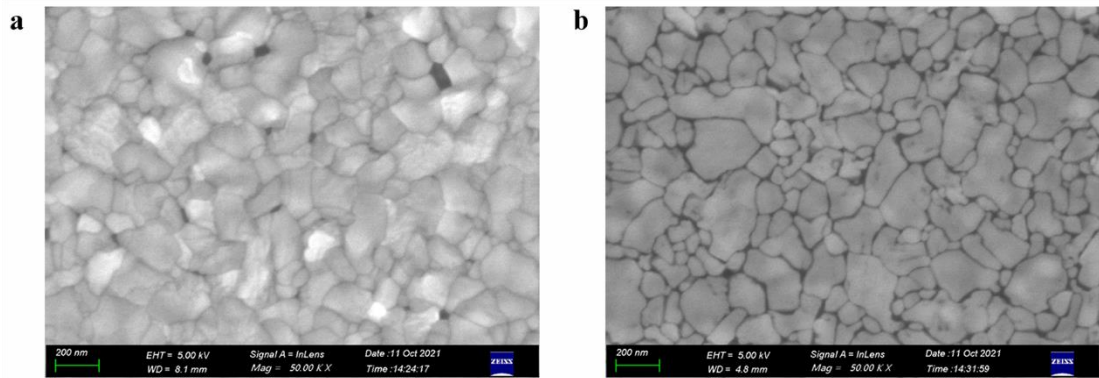| phDMADBr concentration (%)	L$_{max}$ (cd m^{-2})	max. CE (cd A^{-1})	V$_{on}$ (V)
Standard	6798.9 at 6 V	0.67	2.4
0.022	11845 at 5.2 V	0.94	2.2
0.044	16329 at 5.6 V	1.14	2.3
0.087	20494 at 6 V	1.35	2.2
0.17	6121.7 at 5.9 V	0.72	2.5
0.26	3592 at 4.7 V	0.52	2.5

Figure S5 CsPbBr$_3$ perovskite films with a concentration of 145mg ml^{-1} (a) without (standard), (b) with 0.5% phDMADBr. The two NH$_3^+$ terminals makes phDMADBr having a stronger interaction with the all-inorganic perovskite films than the conventional single NH$_3^+$ terminal, so that just a small ratio can passivate the defects effectively. However, a big ratio of phDMADBr will damage the film. The excess phDMADBr will fill in the grain boundary (**Figure S5b**), and cause a decrease to the device performance. The results are entirely consistent with the experiment and DFT calculations in this work.
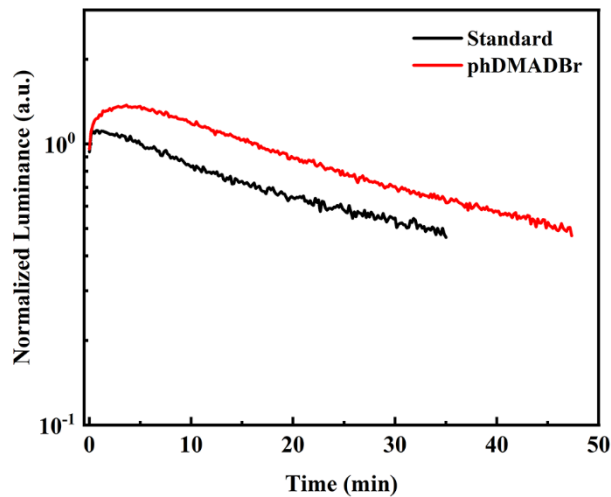

Figure S6 Operation stability properties of PeLEDs based on without (standard) and with

phDMADBr modification in atmosphere condition.